D1

Rapid regionally restricted pH_i shifts inneurones induced by the UV photolysis of 2-nitrobenzaldehyde

Christof J. Schwiening

Department of Physiology, University of Cambridge, DowningStreet, Cambridge CB2 3EG, UK

Hitherto three types of techniques have been used to changeintracellular pH (pH_i): superfusion of weak acids or bases (Jacobs, 1920), cytosolic injection of acid or alkali, or the activation of channels or transporters (e.g. the Ca^{2+}:H^+ pump, Schwiening *et al.* 1993) that allow transmembrane H^+ or HCO_3^- fluxes. Here I describe a fourth technique, the regional UV-induced release ofprotons (Ciamician & Silber, 1901; George & Scaiano, 1980) that allows for extremely rapid and localized acidic pH_i shifts. This technique should provide a simple, cheap and highly controllable way of generating local pH_i signals independently of changes in other ion concentrations (e.g. Ca^{2+}).

Helix aspersa neurones were isolated from the gangliafollowing enzymatic digestion and mechanical agitation (Schwiening & Willoughby, 2002). Snail Ringer solution containing the isolated neurones was placed in a superfusion chamber on a Zeiss LSM 510 confocal microscope and the cells were allowed to settle for ~1 h. A cell with an axonal projection was selected and patch clamped in the whole-cell configuration (pipettes ~1.5 μm tip filled with 110 mM CsCl, 0.5 mM of the pH-sensitive dye HPTS). pH-sensitive fluorescence was imaged (488 nm excitation, 505 nm emission) using a 63x water-immersion c-apochromat objective (1.2 NA). In some experiments ratiometric pH recordings were made using alternating 488 nmand 357 nm excitation of the dye HPTS. 2-nitrobenzaldehyde (NBA; Sigma-Aldrich) was bath applied at between 1.0 and 10 mM (made up fresh each day from a 100 mM stock solution in methanol) and uncaged using the LSM510 bleach function (AOTF-modulated illumination with 364 nm light during a whole image sweep) at maximum power.

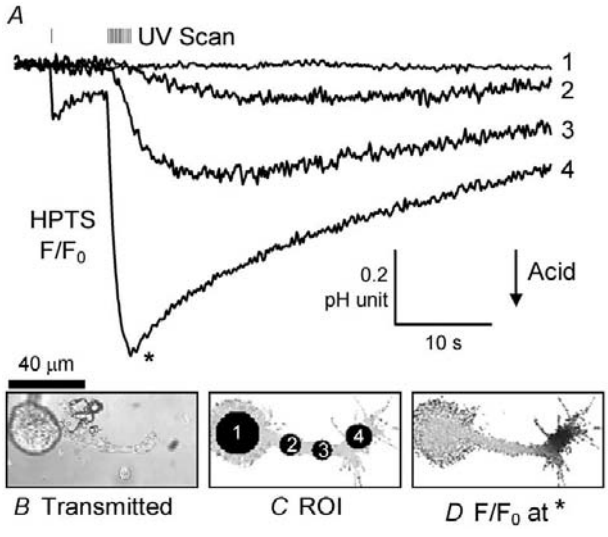

Figure 1. *A*, pH-sensitive fluorescence plotted from four regions of interest (ROI; see Fig. 1*C*) of an isolated snail neurone bathed in snail Ringer containing 2 mM NBA. NBA was photolysed in region 4 (the axon foot), during a whole image sweep (55 ms frame^{-1}, dwell time 9.85 μs μm^{-2}), at the times indicated in the UV scan trace. The first uncaging of H^+ was induced by one sweep of the UV laser, whilst the second consisted of 13 discrete sweeps over 2.15 s. *B*, image of the snail neurone (128 × 67 pixels) with tip of patch pipette top left. *C*, confocal F/F_0 image before acidification showing the four ROI plotted in A. *D*, confocal F/F_0 image at the peak (*) of the acidification (average of 18 images).

Spatially restricited acidic pH_i shifts, induced by the flash release of acid, are shown at low magnification in Fig. 1, and at higher magnification in Fig. 2. In both cases NBA was applied several min before the start of the trace. NBA appears to be highlymembrane permeant since prolonged illumination with UV light yields a larger change in pH_i (~0.8 pH unit) than expected from the complete releaseof 2 mM H^+ with a buffering power of 10 mM H^+ (l cell volume)$^{-1}$. Also, when bath applied, NBA diffuses rapidly into the cell as judged by the appearance of UV-induced pH_i shifts. It isunlikely that HPTS photobleaching underlies the F/F_0 changes presented here since UV illumination in the absence of NBA did not produce anychange in HPTS fluorescence, furthermore ratiometric recording of pH using HPTS produced similar results to the single wavelength records shown here.

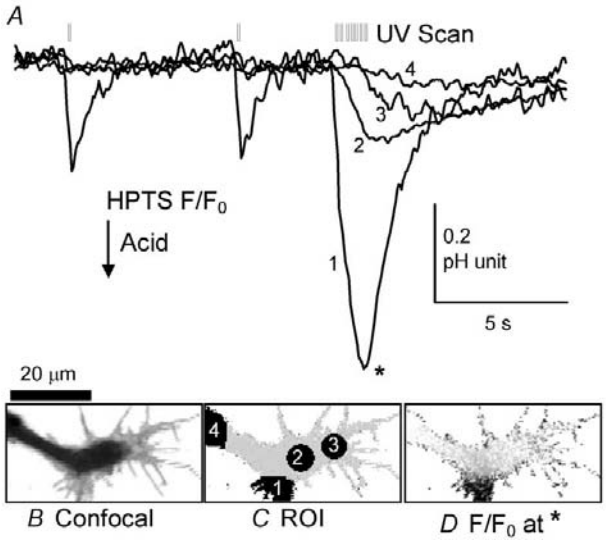

Figure 2. *A*, pH-sensitive fluorescence recorded in the axon foot region of the cell shown in Fig. 1*B*. Two single UV illuminations (dwell time 39 μs μm^{-2}) were followed by a series of 7 illuminations over 1s. *B*, confocal image of axon foot (128 × 67 pixels). *C*, confocal F/F_0 image before acidifications showing the four ROI plotted in *A*. *D*, confocal F/F_0 image at the peak of the acidification.

This demonstration is, to the best of my knowledge, thefirst time acid has been both locally flash released and recorded inside a cell. Such release of intracellular acid is by far the most rapid and controllable method for altering regional pH_i. Photolysis of NBA, orits derivatives (Abbruzzetti *et al.* 2003), should facilitate the investigation pH_i microdomain signalling targets in normal neuronalfunction.

Ciamician GL & Silber P, (1901). *Ber Dtsch Chem Ges* **34**, 2040–2046.

George MV & Scaiano JC, (1980). *J Phys Chem* **84**, 492 – 495.

Jacobs MH (1920). *Am J Physiol* **53**, 457–463.

Schwiening CJ *et al.* (1993). *Proc Roy Soc Lond B* **253**, 285–289.

Schwiening CJ & Willoughby D (2002). *J Physiol* **538**, 371–382.

I thank the MRC for providing the LSM510 and their high rating of my recent grant applications. However, I deplore their failure to support any of my current work, including that presented here, which has been supported by the University.

C37

Inputs to the suprachiasmatic nucleus from the arcuate nucleus are modulated by leptin

A.N. Inyushkin and R.E.J. Dyball

Department of Anatomy, University of Cambridge, Cambridge CB2 3DY, UK

The hypothalamic suprachiasmatic nucleus (SCN, the clock nucleus) is a part of a network regulating feeding and metabolism. The hypothalamic arcuate nucleus (ARCN) may be involved in food intake regulation while the SCN modulates the timing of feeding. The input to the SCN from the retrochiasmatic area of the ARCN provides a route by which the SCN may be influenced by neuroendocrine cues. The SCN has been reported to contain receptors to leptin (Hakansson *et al.* 1998), the peptide secreted by adipose tissue and involved in the modulation of the neural control of feeding. The aim of the present study was to determine if leptin influenced the activity of cells in the SCN or their responses to stimulation of the ARCN.

Conventional extracellular recordings were made from single units in the SCN in 500 μm sagittal hypothalamic slices of brains removed from anaesthetised (urethane 1.2 g/kg I.P.) male Wistar rats and their responses to ARCN stimulation were assessed by peristimulus time histograms.

A total of 24 of the 35 SCN cells responded to stimulation of the ARCN. Excitatory ($n = 12$), inhibitory ($n = 7$), and complex responses (excitation followed by inhibition or vice versa; $n = 5$) were seen. The responses had a short latency (< 20 ms) after the stimulus pulse. Typically excitatory responses had a short duration ($\leqslant$25 ms) and inhibitory responses were longer ($\geqslant$40 ms). After the administration of leptin (20 nM) the mean spike frequency of SCN cells was reduced ($P < 0.001$, Wilcoxon signed rank test) while mean log interspike interval (ISI) was increased in duration ($P = 0.033$, Wilcoxon signed rank test). The entropy of the log ISI probability distribution was also increased by 0.16 ± 0.07 (mean difference ± S.E.M., $P = 0.033$, paired t test) a change in the regularity of the recorded spike train. The input to the SCN from the ARCN was significantly influenced by leptin in 12 of 35 experiments. Excitatory responses were reduced in 7 cases and increased in 2 cases. In one case an excitatory response became evident only in the presence of leptin. Leptin did not appear to alter inhibitory responses that were seen before its administration but in two experiments inhibitory responses became evident only in the presence of leptin. The effects of leptin developed relatively slowly (> 10 min) and in most cases were completely or partially reversible following washout with control solution for 20–30 min.

The present results show that leptin can influence the activity of SCN units and modulate the input to the SCN from the ARCN. The effects of leptin involved both a change in the regularity of the ISI of the spike trains recorded from SCN neurons and a reduction in their firing rate. The heterogeneity of the responses probably, reflects the diversity of cell types in the SCN.

Hakansson ML *et al.* (1998). *J Neurosci* **18**, 559–572.

This work was supported by the EPSRC.

All procedures accord with current UK legislation

C38

Daily rhythms of spike coding in the suprachiasmatic nucleus

G.S. Bhumbra, K. Saeb-Parsy and R.E.J. Dyball

Department of Anatomy, University of Cambridge, Cambridge CB2 3DY, UK

Although the suprachiasmatic nucleus (SCN) is widely regarded as the main circadian pacemaker in the mammalian brain, evidence for a rhythm of firing activity based on extensive single unit recording in intact animals has been reported only recently (Saeb-Parsy & Dyball, 2003). There were significant differences in mean spike frequency at different times of the day but the differences were not clearly evident unless activity was averaged over arbitrary time epochs. The use of such averaging techniques represents a substantial of loss of information. We have found that parameters that measure the irregularity of spike activity of cells in the SCN show more obvious changes over the day/night cycle than mean spike frequency.

Using a ventral surgical approach, extracellular single unit activity was recorded from SCN cells in urethane (1.2 g/kg I.P.) anaesthetised rats *in vivo*. All rats were killed humanely at the end of the experiments. Conventional variance measures were not used to quantify the variability of inter-spike intervals because of the non-Gaussian distribution of the intervals. To measure the irregularity of spike activity, we used the entropy (a widely used measure of disorder) of the log interval distribution. Such a measure quantifies the variability of intervals and thus the coding capacity of each spike. The entropy was plotted against the respective zeitgeber and showed an oscillation that could be described using a second order Fourier expansion with a peak in the mid-dark period.

Neurones within the SCN showed a significant rhythm in entropy ($n = 166$; $P < 0.001$) and there was a similar rhythm in the activity of cells recorded from perinuclear zone (PSCN) of the suprachiasmatic nucleus ($n = 209$; $P = 0.0370$). SCN and PSCN cells with caudal projections showed a significant rhythm ($n = 78$; $P = 0.006$) with a peak in the mid-light period whereas those without a caudal projection showed a rhythm with a peak in the mid-dark period ($n = 297$; $P = 0.001$). There was no evidence for a rhythm of activity for hypothalamic more than 1 mm distant from the SCN.

Thus measures of SCN cell activity in addition to mean spike frequency show a daily rhythm that is more obvious. Cells within the SCN show a clearer rhythm than cells in the PSCN and different populations of cells within the SCN show rhythms that appear to be different from each other.

Saeb-Parsy K & Dyball REJ (2003). *J Biol Rhythms* **18**, 26–42.

This work was supported by Merck, Sharp, and Dohme and the James Baird fund.

All procedures accord with current UK legislation

C39

Pinealectomy appears to eliminate the daily rhythm of firing activity in the suprachiasmatic nucleus that is seen in intact animals

J.A. Gonzalez and R.E.J. Dyball

Department of Anatomy, University of Cambridge, Cambridge CB2 3DY, UK

The suprachiasmatic nuclei (SCN) of the hypothalamus are widely regarded as the part of the brain that generates circadian rhythms in mammals. Secretion of the pineal hormone melatonin is one of a number of neuroendocrine events that show a daily rhythm (Perreau-Lenz *et al.* 2003), and melatonin in turn affects the circadian clock by mechanisms that are unclear (Pevet *et al.* 2002). It has recently been demonstrated using single-unit recordings from the SCN in intact animals that SCN cells show a daily rhythm of mean spike frequency (Saeb-Parsy & Dyball, 2003). The present study was undertaken to extend the earlier study and to explore the role played by melatonin in the generation of rhythms in the SCN by making recordings from pinealectomised rats.

Using the ventral surgical approach, single-cell recordings were made in anaesthetised (urethane, 1.2 g/kg I.P.) rats *in vivo* between 3 and 10 weeks after pinealectomy under isofluorane. The rats were killed humanely at the end of the experiments.

In pinealectomised rats, recordings were made from 192 SCN cells at different times of the day night cycle and the activity of each of them, recorded for a minimum of 10 min, was recorded. Activity was expressed both in terms of mean spike frequency and in terms of the entropy of the log interspike interval distribution. The entropy of the log interspike interval distribution quantifies the variability in the interval distribution and thus gives a measure of the coding capacity of each spike. Entropy was plotted against the respective Zeitgeber time. In intact animals such a plot showed an oscillation that could be described using a second order Fourier expansion with a peak in the mid-dark period. Monte-Carlo significance testing showed a significant rhythm in intact animals (Bhumbra *et al.* 2003). In pinealectomised animals, however, the maximum amplitude (0.4092 bits) of the curve describing the SCN cell activity was below the amplitude found after fitting the corresponding curves to randomised data (maximum amplitude after 10,000 randomisations, 0.8139 bits), and thus the oscillation seen in real data was not statistically different from a flat line ($P < 0.001$, Monte-Carlo significance testing). Therefore, after pinealectomy no rhythm in the activity of the SCN cells with the dark/light period was detected. Mean spike frequency showed a similar lack of change in pinealectomised animals. It thus appears that at least some aspects of the rhythmic activity of the SCN do not persist after pinealectomy.

Bhumbra GS *et al.* (2003). *J Physiol. This meeting.*

Perreau-Lenz S *et al.* (2003). *Eur J Neurosci* **17**, 221–8.

Pevet P *et al.* (2002). *Cell Tissue Res* **309**, 183–91.

Saeb-Parsy K & Dyball REJ (2003). *J Biol Rhythms* **18**, 26–42.

This work was supported by St John's College, Cambridge.

All procedures accord with current UK legislation

C40

Microamperometric recording of noradrenaline release from visualised axonal varicosities of A1 noradrenergic neurones

A.G. Teschemacher

Department of Pharmacology, School of Medical Sciences, University of Bristol, University Walk, Bristol BS8 1TD, UK

The characteristics of noradrenaline (NA) release from central neurones have largely been inferred from experiments in model systems such as bovine adrenal chromaffin cells or the PC12 cell line (Ninomiya *et al.* 1997;Teschemacher & Seward, 2000). In these models it is possible to place microamperometric electrodes on individual cells and monitor exocytosis of NA. Similar experiments in native brain noradrenergic (NAergic) neurones have not been possible because the release sites are difficult to visualise and access. We have developed a method which allows direct recording of NA release from NAergic neurones from specific brainstem nuclei.

To this end organotypic brainstem slice cultures are prepared from humanely killed 9-day-old rats. Cultures are subsequently transfected with an adenoviral vector which causes expression of EGFP selectively in NAergic neurones under the control of an artificial promoter (PRSx8; Hwang *et al.* 2001). After >3 days, clusters of fluorescent neurones can be visualised using conventional epifluorescence and confocal microscopy in living slices in the areas consistent with the location of the known brainstem NAergic and adrenergic cell groups (A1, A2, A6, C1). In addition to cell bodies, multiple processes including characteristic beaded axons can be traced for hundreds of micrometers. These axons were approached by microamperometric probes (5 μm tip diameter). Oxidative current spikes were detected as described for vesicular catecholamine release in isolated cell models. This method will be used to study modulation of NA release from the different cellular compartments of identified NAergic neurones and can be combined with further genetic manipulation of the same cells.

Hwang D-Y *et al.* (2001). *Human Gene Ther* **12**, 1731–1740.

Ninomiya Y *et al.* (1997). *EMBO J* **16**, 929–934.

Teschemacher AG & Seward EP (2000). *J Neurosci* **20**, 4776–4785.

This work was supported by the Royal Society (23697), and BBSRC (7/JE616459)

All procedures accord with current UK legislation

C42

Clathrin-mediated retrieval of vesicles at hippocampal synapses

Stephen J. Royle and Leon Lagnado

MRC Laboratory of Molecular Biology, Hills Road, Cambridge CB2 2QH, UK

Exocytosis of neurotransmitter from a synaptic vesicle is followed by efficient retrieval of its constituent membrane and proteins. Several different mechanisms of endocytosis occur at synapses, but their relative importance has been unclear (Royle & Lagnado, 2003). We have investigated the role of clathrin-mediated endocytosis (CME) by using RNA interference (RNAi) to selectively knock-down the expression of clathrin heavy chain (CHC) in hippocampal neurons.

Primary cultures of rat hippocampal neurons were prepared

from E19 pups and all animals were humanely killed. Exocytosis and endocytosis were measured by confocal imaging of the optical probe synapto-pHluorin (SpH), which is quenched at the acidic pH within synaptic vesicles (Sankaranarayanan *et al.* 2000) and the styryl dye FM4–64. RNAi was achieved by transfection of short interfering RNAs (siRNAs).

At 72 h post-transfection the expression of CHC was reduced to 10.6 ± 0.8 % compared to control neurons (mean ± S.E.M.) and transferrin uptake by CME was reduced to 38.6 ± 0.9 %. Depolarization for 60 s by local perfusion of hyperkalaemic saline caused an increase in SpH fluorescence, reflecting exocytosis. SpH fluorescence then decayed back to resting levels, reflecting retrieval of the probe from the membrane surface into acidified organelles (Sankaranarayanan *et al.* 2000). In control neurons transfected with scrambled siRNA, SpH fluorescence increased 4-fold on stimulation and recovery was complete within 3–4 mins (220 boutons in 7 neurons). In neurons in which CHC was knocked-down, the exocytic response was inhibited in 83 % of boutons and there was little or no recovery over the 5 mins following exocytosis (210 boutons in 12 neurons). In separate experiments, FM4–64 (15 μM) was applied in the hyperkalaemic saline and then washed off to stain any vesicles that were internalised. Synaptic boutons in control neurons stained brightly, but the dye was not internalized by boutons of neurons in which CHC was knocked down.

These findings suggest that CME plays an important role in the retrieval of synaptic vesicles at the synapse. Inhibition of CME also leads to a reduction in the number of vesicles available for exocytosis.

Royle S & Lagnado L (2003). *J Physiol* **553**, 345–355.

Sankaranarayanan S *et al.* (2000). *Biophys J* **79**, 2199–208.

This work was supported by the Human Frontiers Science Program (HFSP)

All procedures accord with current UK legislation

C43

A role for peroxisome proliferator activated receptors in the β-amyloid (A$\beta_{[1–40]}$) mediated impairment of hippocampal long-term potentiation *in vitro*

D.A. Costello and C.E. Herron

Department Physiology, Conway Institute, UCD, Ireland

Alzheimer's disease (AD) is a neurodegenerative disorder associated with accumulation of the β-amyloid peptide (Aβ). Aβ has been shown to impair hippocampal long-term potentiation (LTP) *in vivo* and *in vitro* (Freir *et al.* 2003; Costello & Herron, 2003). LTP is an activity-dependent increase in synaptic efficacy, widely accepted as a cellular model of memory. Peroxisome proliferator activated receptors (PPARs) are a class of nuclear receptor transcription factors, regulated by mitogen activated protein kinases (MAPKs). PPARγ expression is elevated in AD (Kitamura *et al.* 1999), and PPAR agonists have been shown to prevent Aβ-stimulated activation of microglia and production of proinflammatory cytokines (Combs *et al.* 2000). We have identified a role for MAPKs in the depressant effects of Aβ on LTP *in vitro* (Costello & Herron, 2003). Here we investigate the effects of PPARγ agonists on synaptic transmission and on the Aβ[1–40]-mediated impairment of LTP.

Experiments were performed on hippocampal slices (350 μm) from humanely killed male Wistar rats (50–100g). The Schaffer collateral-commissural pathway was stimulated at 0.033 Hz and field excitatory postsynaptic potentials (EPSPs) were recorded in area CA1. LTP was induced by applying high frequency stimuli (HFS; 10 trains of 10 pulses at 200 Hz, repeated 3 times at 20 s intervals). Control LTP was recorded 1 h post-HFS (167 ± 4 %, %EPSP slope ± S.E.M., $n = 8$).

Aβ[1–40] (200 nM) significantly reduced LTP (137 ± 6%, $n = 5$, $P < 0.001$ repeated measures ANOVA), when applied 1 h pre-HFS. The PPARγ agonist troglitazone (20 μM) significantly enhanced LTP (174 ± 10 %, $n = 5$, $P < 0.05$), when applied 30 min prior to HFS. Ciglitazone (20 μM) however did not affect LTP significantly (161 ± 9 %, $n = 4$), but enhanced baseline transmission (108 ± 4 %, $n = 4$, $P < 0.05$) 30 min following application. The endogenous PPARγ agonist, 15-deoxy-$\Delta^{12,14}$PGJ$_2$ (5 μM), reduced LTP significantly (143 ± 2 %, $n = 5$, $P < 0.001$), but also increased baseline transmission (109 ± 3 %, $n = 5$, $P < 0.05$) when present for 30 min. When slices were perfused with each agonist for 30 min and A$\beta_{[1–40]}$ for a further 60 min, the depression in LTP was significantly attenuated when compared with A$\beta_{[1–40]}$ alone (troglitazone+Aβ: 163 ± 5 %, $n = 5$, $P < 0.005$; ciglitazone+Aβ: 152 ± 9 %, $n = 5$, $P < 0.0001$; PGJ$_2$ +Aβ: 164 ± 9 %, $n = 4$, $P < 0.05$), measured 1 h post-HFS. However, in the presence of ciglitazone and A$\beta_{[1–40]}$, LTP did not differ significantly compared with control values or A$\beta_{[1–40]}$ alone (152 ± 9%, $n = 5$). This suggests that enhancing PPARγ activity may reduce the impairment of LTP mediated by A$\beta_{[1–40]}$. We also suggest involvement of PPARγ agonist in the regulation of synaptic transmission and LTP in the CA1.

Combs CK *et al.* (2000). *J Neurosci* **20**, 588–567.

Costello DA & Herron CE (2003). *J Physiol* 547P.

Freir DB *et al.* (2003). *J Neurophysiol* **89**, 3061–3069.

Kitamura Y *et al.* (1999). *Biochem Biophys Res Commun* **27**, 582–586.

This work was supported by HRB Ireland and Enterprise Ireland

All procedures accord with current national and local guidelines

---

C44

Disrupted synaptic transmission in hippocampal slices taken from aged TAS10 mice

J.T. Brown, J.C. Richardson, A.D. Randall and C.H. Davies

Neurology & GI Centre of Excellence for Drug Discovery, GlaxoSmithKline, New Frontiers Science Park, Third Ave, Harlow, Essex CM19 5AW, UK

Transgenic mice overexpressing amyloid precursor protein (APP) have previously been shown to have deficits in either hippocampal basal synaptic transmission (Fitzjohn *et al.* 2001) or synaptic plasticity (Chapman *et al.* 1999) but not both. We have studied synaptic transmission and plasticity in hippocampal slices taken from aged (12–14 months) TAS10 mice (Richardson *et al.* 2003) overexpressing APP harbouring the Swedish mutation (K670N and M671L), in an attempt to resolve these confounding reports. In addition, we have examined neuronal network behaviour induced by 4-aminopyridine (4-AP).

Wildtype (WT) and heterozygous transgenic mice (male and female) were killed humanely and 400 μm-thick horizontal hippocampal slices prepared in a standard manner. Data are presented as mean ± S.E.M. and statistical significance determined using Student's unpaired t test, unless otherwise stated.

In TAS10 slices we observed a significant deficit in basal synaptic transmission in the CA3-CA1 Schaffer collateral pathway such that the mean ratio of the slope of the maximal fEPSP to fibre volley amplitude was approximately six-fold lower (0.63 ± 0.14, $n = 14$) than in WT slices (3.27 ± 0.55, $n = 11$; $P < 0.001$). Despite this deficit, relative levels of short-term synaptic

plasticity in the CA1 region of TAS10 slices (paired pulse and multiple pulse facilitation, at frequencies of 1, 5 and 10 Hz) were normal. In addition, LTP induced by a theta burst stimulation paradigm, was normal in the CA1 of TAS10 slices (WT = 160 ± 12 % of baseline, $n = 8$; TAS10 = 186 ± 10 % of baseline, $n = 8$, $P > 0.05$ 2-way ANOVA). The inter-event interval (IEI) of synchronous events induced by 100 μM 4-AP was significantly longer in TAS10 hippocampal slices (IEI, 6.9 ± 1.7 s; $n = 8$) compared with WT slices (IEI, 2.4 ± 0.6 s; $n = 6$, $P < 0.05$). Addition of NBQX (20 μM) and D-AP5 (50 μM) to the bath medium, isolated bicuculline-sensitive GABA-mediated synchronous events in both WT and TAS10 slices. These GABAergic events were similar in frequency in WT and TAS10 slices (IEI, 10.3 ± 1.2 s in WT slices cf. 10.8 ± 1.3 s in TAS10 slices), suggesting that GABAergic systems remain relatively unaffected by overproduction of β-amyloid.

This study suggests that the deficit in glutamatergic synaptic transmission, observed in several strains of APP overexpressing mice, may be coupled with alterations in synchronous network activity, which in turn may lead to deficient information processing.

Chapman *et al.* (1999). *Nat Neurosci* **2**, 271–6.
Fitzjohn *et al.* (2001). *J Neurosci* **21**, 4691–8.
Richardson *et al.* (2003). *Neuroscience* (in press).

All procedures accord with current UK legislation

C45

The latency to the anoxic depolarization of CA1 pyramidal cells in rat hippocampal slices exposed to different types of metabolic inhibition

Ragnhildur Káradóttir, Nicola J. Allen and David Attwell

Department Physiology, University College London, Gower Street, London WC1E 6BT, UK

During brain anoxia or ischaemia a fall of ATP level leads to a sudden run-down of transmembrane ion gradients (the anoxic depolarization or AD). This releases glutamate by reversed uptake (Rossi *et al.* 2000), which triggers the death of neurons. By whole-cell clamping pyramidal cells (using a KCl-based, BAPTA and ATP containing internal solution) to sense the rise of $[glutamate]_o$ accompanying the AD, we have investigated the energetic factors controlling the latency of the AD in area CA1 of hippocampal slices (from P12 rats killed humanely by cervical dislocation).

When oxygen and glucose (10 mM) were removed, glycolytic ATP production was blocked with iodoacetate (2 mM), and mitochondrial ATP production was blocked using rotenone (100 μM) and antimycin (100 μM), the AD occurred in ~7.5 mins (440 ± 17 (S.E.M.) s $n = 29$) at 33 °C. Allowing glycolysis fuelled by glycogen, when glucose and oxygen were removed and mitochondria were blocked, delayed the AD by a further ~5.5 mins (to 771 ± 37 s $n = 8$), and if external glucose was present the AD was prevented altogether (latency > 3922 ± 811 s $n = 4$). Allowing mitochondria to function when glycolysis was blocked increased the latency to the AD by over 6 mins (786 ± 78 s $n = 13$, compared with 409 ± 37 s $n = 7$, when mitochondria were blocked, both experiments done with oxygen present, glucose removed and iodoacetate added), suggesting that metabolites feeding mitochondria downstream of glycolysis (pyruvate and citric acid cycle intermediates) provide a significant energy store. Superfusing lactate (5 mM) in this situation did not prevent the AD occurring, and provided no extra increase in the latency to the AD ($n = 7$). Simply removing oxygen and glucose from the superfusion solution produced an AD after 17 mins (1021 ± 84 s $n = 5$). By comparison *in vivo* ischaemia produces an AD after ~2 mins, implying a ~3 mins latency at the 33 °C used here.

These data show that glycolysis alone can prevent the anoxic depolarization, and do not support the idea that most brain ATP production is powered by lactate supplied to neurons by glia. The long latency to the AD seen on simply removing oxygen and glucose may result from: (i) the presence of residual oxygen in superfusion solutions passing through the recording chamber, which has to be open to the air to allow electrode access; (ii) a lower metabolic rate for sliced tissue compared to tissue *in vivo*; (iii) the use of a non-physiologically high glucose concentration (10 mM) which gives the tissue an abnormally high reserve of glycogen.

Rossi DJ Oshima T & Attwell D (2000). *Nature* **403**, 316–321.

NA and RK are in the 4 year PhD Programme in Neuroscience at UCL. This work was supported by the Wellcome Trust, the EU and a Wolfson-Royal Society award.

All procedures accord with current UK legislation

C46

Tonic release of glutamate in rat hippocampal slices by a DIDS-sensitive mechanism

Pauline Cavelier and David Attwell

Department of Physiology, University College London, Gower Street, London WC1E 6BT, UK

Tonic release of glutamate into the extracellular space of the hippocampus and striatum has been attributed to a cystine-glutamate exchanger which is blockable by the glutamate analogue CPG, and adaptation of this release in the striatum has been suggested to underlie relapse in the use of cocaine (Jabaudon *et al.* 1999; Baker *et al.* 2002, 2003). We monitored tonic glutamate release in area CA1 of hippocampal slices (from P12 rats killed humanely by cervical dislocation) by using whole-cell patch-clamping to measure the glutamate receptor mediated current evoked in pyramidal cells when Na-dependent glutamate uptake was blocked with the non-transported glutamate analogue TBOA (200 μM). The superfusion solution contained TTX (0.1–1μM) to block action potentials.

TBOA evoked a slowly developing inward current at −30 mV which reached ~125 pA after 1.5 mins, and was abolished by the NMDA receptor blocker D-AP5 (50 μM). The TBOA-evoked current was not significantly affected by CPG (50μM), even though cystine (300 μM) increased the TBOA-evoked current 2.8 ± 1.9 fold (mean ± S.E.M., $P = 0.04$ by 2 tailed t test, $n = 5$,) and sometimes evoked an inward current even in the absence of TBOA (as seen previously in cerebellum and cortex: Warr *et al.* 1999), demonstrating that cystine-glutamate exchange is present in area CA1. The TBOA-evoked current was reduced by 49 ± 11 % ($P = 0.0004$, $n = 5$) by DIDS (1 mM). DIDS has been claimed to block NMDA receptor mediated currents (Tauskela *et al.* 2003), but this was found to be an artefact (produced by the co-application of NMDA and DIDS) reflecting the superposition of a DIDS-evoked outward current on an NMDA-evoked inward current.

These data suggest that although cystine-glutamate exchange is present in the hippocampus it does not generate the tonic release of glutamate, and that the tonic release is mediated by a DIDS-sensitive mechanism.

Baker DA *et al.* (2002). *J Neurosci* **22**, 9134–9141.
Baker DA *et al.* (2003). *Nature Neurosci* **6**, 743–749.

Jabaudon D *et al.* (1999). *Proc Natl Acad Sci U S A* **96**, 8733–8738.
Tauskela JS *et al.* (2003). *Eur J Pharm* **464**, 17–25.
Warr O Takahasi M & Attwell D (1999). *J Physiol* **514**, 783–793.

This work was supported by the Wellcome Trust, the European Union and a Wolfson-Royal Society Award.

All procedures accord with current UK legislation

C47

Glutamate spillover and activation of mGluR1 in mouse cerebellar Purkinje cells

Paikan Marcaggi and David Attwell

Department of Physiology, University College London, Gower Street, London WC1E 6BT, UK

At the cerebellar parallel fibre to Purkinje cell synapse, repetitive stimulation of a beam of parallel fibers evokes a fast AMPA receptor mediated synaptic current (EPSCfast), and a slow synaptic current (EPSCslow) mediated by metabotropic glutamate (mGluR1) receptors (Tempia *et al.* 1998). Here we examine how the EPSCslow magnitude depends on the number of activated synapses, which was determined from the size of the EPSCfast (in GABAzine, 100 μM) evoked by different stimulus strengths (Marcaggi *et al.* 2003).

We recorded from Purkinje cells in sagittal cerebellar slices from 2–3 week old mice killed humanely by cervical dislocation. Cells were clamped at −70 mV and the internal medium was Cs-gluconate based with 0.1 mM $CaCl_2$ buffered by 0.5 mM EGTA at pH 7.3. Stimulating in the molecular layer (10 pulses at 200 Hz), we observed a supralinear dependence of the amplitude of EPSCslow on the number of activated synapses, implying an interaction between different synapses. We previously showed that the AMPA receptor mediated EPSC was prolonged when more synapses were activated (again implying interaction between synapses), and that this prolongation was mimicked and amplified by inhibition of glial glutamate transporters, suggesting that it was due to glutamate spillover (Marcaggi *et al.* 2003). Knock-out of the main glial glutamate transporter GLAST approximately doubled the EPSCslow amplitude, and superimposed inhibition of GLT-1 by dihydrokainate further doubled the amplitude. In wild-type slices, superfused with solution containing the broad spectrum glutamate transporter blocker TBOA, when parallel fibres passing close to, but not contacting, the recorded cell were stimulated an EPSCslow could be detected, showing that spillover of glutamate could, in these conditions, elicit an EPSCslow. When stimulation was applied to the granular layer or white matter, rather than the molecular layer, so that activated synapses were more scattered in the Purkinje cell dendritic tree, the EPSCslow was approximately 1/3 of the size of the EPSCslow induced by molecular layer stimulation of the same number of synapses.

We conclude that the EPSCslow is strongly shaped by glial glutamate uptake and by the spatial arrangement of activated synapses on the Purkinje cell dendritic tree.

Marcaggi P *et al.* (2003). *J Physiol* (in press).
Tempia F *et al.* (1998). *J Neurophysiol* **80**, 520–528.

This work was supported by the European Union, the Wellcome Trust and a Wolfson-Royal Society award. We thank Prof K. Tanaka for the GLAST KO mice.

All procedures accord with current UK legislation

C49

Effect of channel noise on the propagating AP wave form and its potential impact on synaptic transmission

A. Aldo Faisal and Simon B. Laughlin

Department of Zoology, University of Cambridge, Cambridge CB2 3AP Cambridge, UK

The action potential (AP) propagates by the concerted action of voltage-gated ion channels, whose probabilistic behaviour introduces channel noise. In thin unmyelinated axons, typical for the mammalian cortex (av o.d. 0.3 μm), channel noise jitters the timing of APs (Faisal *et al.* 2002), generates spontaneous APs (Faisal *et al.* submitted) and varies the AP wave form. The wave form of the presynaptic AP is of fundamental importance in determining the strength of synaptic transmission (e.g. Sabatini & Regehr (1997)). However, the variability of the AP wave form in thin axons is unknown, because it is difficult to record fast signals from within such small structures.

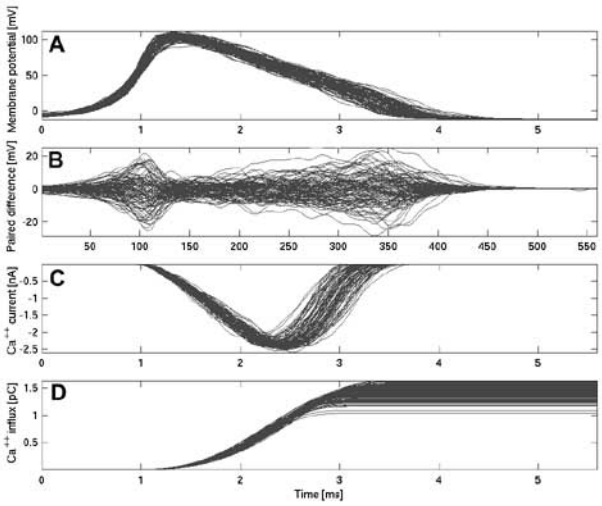

Figure 1. *A*, superposition of $n = 100$ subsequent AP arriving at the axon terminal (95 % of axon length). *B*, superposition of differences between wave form measured at 50 % and 95 % of axon length of the above APs. *C*, superposition of Ca^{2+} currents and *D*, Ca^{2+} ion influx resulting from the above APs invading a Calyx-of-Held type synapse model. See text for parameters and model used.

We developed a stochastic simulator and simulated a 1.6 mm long unmyelinated pyramidal cell axon collateral of 0.2 μm diameter (Na and K channel densities 60 μm^{-2} and 18 μm^{-2}, channel conductance 20 pS, $R_a = 70\ \Omega$ cm, $R_m = 20000\ \Omega\ cm^2$, resting potential −65 mV), which was stimulated with white noise current (0 nA ± 0.01 nA) at its proximal end. The travelling AP wave form fluctuated considerably (Fig. 1, $n = 713$). AP width (at half-peak) measured mid-way down the axon and at its terminal had coefficients of variation (CV = S.D./av) of 8 % (1.6 ms ± 0.11 ms S.D.) and AP height (resting potential to peak) had CVs of 4 % (103 mV ± 4.5 mV). Individual APs showed only weak correlation in their wave forms at mid-axon and the terminal end (correl coef 0.08 and 0.05 for AP width and height). Thus, wave form variability results from channel noise and not from the stimulus. To determine how form variability affects post-synaptic responses, we compared it to data from a variety of large synapses. These show consistently a linear relationship between AP width and EPSC amplitude. A CV in AP width of 8 % would translate e.g. for a Granule Cell to Purkinje Cell synapse (Sabatini & Regehr, 1997) into a CV of

50 % for the EPSC amplitude. The AP wave form determines the calcium signal that controls vesicle fusion, by both controlling the opening of voltage-gated calcium channels and the driving force for calcium influx. Integrating our simulated AP wave forms into a model of a Calyx-of-Held type synapse (Borst & Sakmann, 1998) shows that both calcium peak current and total calcium ion influx have a CV of 9 %, which translates (Augustine, 2001) into a change in vesicle release probability of over an order of magnitude. Synaptic reliability and variability has been in general attributed to mechanisms inside the cortical synapse, but our knowledge is based on paired soma recordings. Thus, it is difficult to dissociate synaptic and axonal stochastic effects. Although care has to be taken when relating data from large synapses to much smaller cortical synapses, our simulations suggest that axonal channel noise could have an impact on cortical synaptic transmission.

Augustine GJ (2001). *Curr Opin Neurobiol* **11**, 320–326.

Borst JG & Sakmann B (1998). *JPhysiol* **503**, 143–157.

Faisal AA *et al.* (2002). *IEEE WCCI 2002 proceedings* **1**, 1661–1669.

Faisal AA *et al.* (2004). *Science* (submitted).

Sabatini BL & Regehr WG (1997). *JNeurosci* **17**, 3425–3435.

AAF is a Boehringer-Ingelheim Fonds Ph.D. Fellow, a BBSRC supported research student and a honorary scholar of the Studienstiftung des deutschen Volkes.

C50

A tonic glycine receptor-mediated current in lateral superior olive (LSO) neurones of the young rat

V.J. Barnes*, M.M. Usowicz*, C.H. Davies† and A.D. Randall†

** Department Pharmacology, University of Bristol, School of Medical Sciences, BS8 1TD and † Neurology & GI CEDD, GlaxoSmithKline, Harlow, Essex CM19 5AW, UK*

Much inhibitory synaptic transmission in the spinal cord and brain stem is mediated by the glycinergic system which classically generates fast, chloride-mediated, inhibitory postsynaptic responses. Here we describe the co-existence of a tonic glycine receptor-mediated conductance with phasic glycine receptor-mediated IPSCs, in neurones of the LSO, and its regulation by glycine transporters.

Brain stem slices (~175 μm) containing the LSO were prepared by standard means from P8-P13 male Lister-hooded rats killed humanely. Whole-cell voltage-clamp recordings (−70 mV, ~35°C) were made from visualised LSO neurones with CsCl-containing pipettes. Data are presented as mean ± S.E.M. Statistical significance was assessed with paired Student's *t* tests.

Under control conditions, spontaneous inward-going synaptic currents with a broad range of amplitudes and kinetic profiles were observed. The frequency of events was decreased by 70 ± 9 % following blockade of glutamate receptor-mediated EPSCs with NBQX (10 μM) and D-AP5 (50 μM), and $GABA_A$ receptor-mediated IPSCs with SR95531 (10 μM). The remaining population of spontaneous currents arose with a median inter-event interval of 1.18 ± 0.17 s and had a median amplitude of −50 ± 6 pA ($n = 11$). These currents had a median 10–90 % rise time of 0.6 ± 0.1 ms and decayed exponentially with a median time constant of 2.7 ± 0.3 ms ($n = 11$). Event frequency was insensitive to TTX (1 μM), but all events were eliminated by the glycine antagonist strychnine (2 μM). Strychnine also decreased both the mean steady-state holding current −128 ± 14 pA control;−113 ± 15 pA, strychnine, $P < 0.02$) and its variance (24.1 ± 3.9 pA2, control; 12.9 ± 2.1 pA2, strychnine, $P < 0.02$). An inhibitor of the type 1 glycine transporter, ALX5407, produced large, strychnine-sensitive increases in both holding current −150.8 ± 18.5 pA, control;−309.3 ± 45.9 pA, ALX5407, $n = 10$, $P = 0.001$) and variance (51.9 ± 9.4 pA2, control; 254.5 ± 31.5 pA2, ALX5407, $n = 10$, $P < 0.001$). An inhibitor of the type 2 glycine transporter, ORG-25543, caused a small increase in holding current that was not statistically significant −167.1 ± 31.2 pA, control;−185.7 ± 35.1 pA, ORG-25543, $P = 0.16$) but did produce a two-fold increase in variance (33.5 ± 5.3 pA2, control; 64.8 ± 7.8 pA2, ORG-25543, $P = 0.002$).

These data demonstrate that LSO neurones receive both phasic and tonic glycinergic inputs, the latter predominantly under control of GlyT1. It will be interesting to determine the roles played by these two forms of inhibition in auditory processing and their relative importance in postnatal development.

All procedures accord with current UK legislation

C51

Morphology, intrinsic firing and synaptic properties of excitatory cells in layer 6 of rat and cat visual cortex

Oliver T. Morris, Audrey Mercer and Alex M. Thomson

Department of Pharmacology, The School of Pharmacy, 29–39 Brunswick Square, London WC1N 1AX, UK

Excitatory cells in layer 6 have diverse morphologies but fall into broad categories according to their long distance projections (Katz, 1987; Zhang & Deschenes, 1997). Corticothalamic cells (CT) have apical dendritic tufts in layer 4 and local axon collaterals arborising in layer 4. Corticocortical cells (CC) are more varied, including short pyramids, inverted pyramids and bipolar cells, but lack apical tufts in layer 4 and have horizontally directed axon collaterals restricted to layers 5/6. These differences suggest distinct roles within the network.

We recorded and filled pairs of layer 6 cells in 450 −500μm slices from 5–6 week old male rats and adult male cats at 34°C (Anaesthesia: halothane + 60 mg kg^{-1} pentobarbitone I.P. for rats; 70 mg kg^{-1} α-chloralose + 6 mg kg^{-1} pentobarbitone I.V. for cats. Animals were humanely killed. Further details in Thomson & West (2003).

Three firing types were observed in rat: tonic (8 cells), phasic (20), and phasitonic (phasic to small suprathreshold depolarisations but tonic to larger depolarisations, 10 cells). Firing type and morphology were correlated: of 17 CT-like cells, most were tonic (8) or phasitonic (6). In contrast, none of 21 CC-like cells was tonic and 17 were phasic. 1037 pairs of layer 6 cells in rat and 141 in cat were tested for synaptic connections, yielding 37 and 8 connections respectively. Average EPSP amplitude (at −72 mV) was 0.73 ± 0.43 mV (mean ± S.D., $n = 22$) and transmission failures ranged from 0 −54 % (12 ± 16 %). Most filled cells had CC-like morphology and phasic firing properties.All connections from CC-like cells exhibited short-term synaptic depression: 2nd EPSP amplitudes were 15 −60 % of the 1st at intervals < 20 ms, recovering to ~80 % at 60 −100 ms. The one connection between CT-like cells recorded had qualitatively different short-term properties, exhibiting clear facilitation (> 150 % at 15 ms interval) and post-tetanic potentiation (EPSPs following 6 spike trains at 3 s intervals were 2.3 those following single spikes).

These data support previous suggestions that CC cells make depressing synaptic connections whereas CT cells make facilitating connections (Beierlein & Connors, 2002; Tarczy-Hornoch *et al.* 1999). The phasic firing properties of CC cells and their depressing synaptic connections are best suited to signalling changes in incoming activity (novelty detection), whereas the ability of CT cells to fire tonically and their less phasic outputs

may enable sustained input both to layer 4 and to the thalamus.

Beierlein M & Connors BW (2002). *J Neurophysiol* **88**, 1924–32.
Katz LC (1987). *J Neurosci* **7**, 1223–49.
Tarczy-Hornoch K *et al.* (1999). *Cereb Cortex* **9**, 833–43.
Thomson AM & West DC (2003). *Cereb Cortex* **13**, 136–43.
Zhang ZW & Deschenes M (1997). *J Neurosci* **17**, 6365–79.

This work was supported by the MRC

All procedures accord with current UK legislation

C52

A selective Na^+ conductance in dexamethasone-treated H441 airway epithelial cells

M.T. Clunes*, A.G. Butt†, R.E.Olver* and S.M. Wilson*

**Lung Membrane Transport Group, Department of Maternal and Child Health Sciences, Ninewells Hospital and Medical School, University of Dundee, Dundee DD1 9SY, Scotland UK and †Department of Physiology, University of Otago, Dunedin, New Zealand*

Airway epithelia absorb Na^+ from the airway surface liquid and this process is vital to lung function, develops in response to increased fetal levels of glucocorticoids, thyroid hormone and adrenaline (reviewed by Olver *et al.* 2004), and is dependent upon epithelial Na^+ channels (Hummler *et al.* 1996). These channels are composed of three subunits (α, β and γ-ENaC) that form a selective Na^+ conductance if co-expressed in Xenopus oocytes. However, several authors have failed to identify such selective Na^+ channels in airway epithelia and Na^+ influx in these cells has thus been attributed to non-selective cation channels, which may be formed by the ENaC subunits in an alternative, stoichiometric arrangement. This prompted us to explore the effects of dexamethasone upon Na^+ conductance in H441 airway epithelial cells.

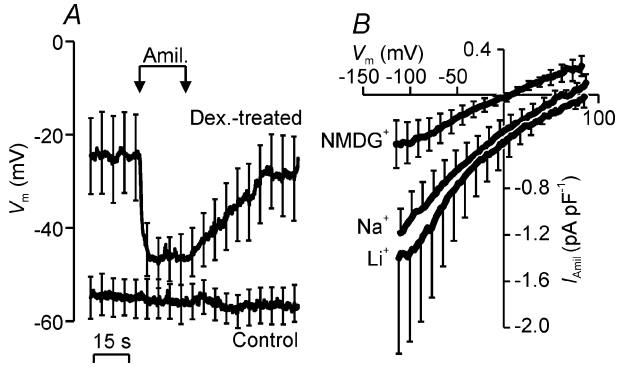

Figure 1. H441 cells were grown (~24 h) on glass coverslips under control conditions or in the presence of 0.2 μM dexamethasone before being studied using the perforated patch technique; all data are mean ± S.E.M. ($n > 4$). *A*, effects of amiloride (10 μM) upon V_m. *B,* the relationship between the amiloride-sensitive current (I_{Amil}) and V_m in dexamethasone-treated cells under quasi-physiological ionic conditions (Na^+) and after abolishing the transmembrane Na^+ gradient by replacing Na^+ with $NMDG^+$ or Li^+.

Measurements of V_m (Fig. 1*A*) showed that dexamethasone caused amiloride-sensitive depolarisation and voltage clamp studies (Fig. 1B) showed that the amiloride-sensitive currents in these cells normally reversed at 65.8 ± 11.8 mV, a potential close to ENa (67.9 mV). Lowering $[Na^+]_o$ to 10 mM, the concentration in the pipette solution, by $NMDG^+$ substitution shifted V_{rev} to 5.3 ± 0.4 mV whilst replacing Na^+ with Li^+ caused a rightward shift in V_{rev} to 90.0 ± 31.8 mV (Fig. 1*B*). Dexamethasone thus evokes the expression of a selective Na^+ conductance with a substantial permeability to Li^+ and this conductance is thus similar to that seen in oocytes co-expressing α, β and γ-ENaC. These data (see also Voilley *et al.* 1994) thus suggest that selective, rather than non-selective, Na^+ channels permit Na^+ entry in airway epithelia.

Hummler E *et al.* (1996). *Nature Genetics* **12**, 325–328.
Olver R *et al.* (2004). *Annu Rev Physiol* (in press).
Voilley N *et al.* (1994). *Proc Natl Acad Sci USA* **91**, 247–251.

This work was supported by grants from the Wellome Trust, Tenovus Scotland and the Dale Fund.

C53

Nociceptor-specific gene deletion using heterozygous $Na_V1.8$-Cre recombinase mice

L. Caroline Stirling, Mohammed A. Nassar, Greta Forlani, Mark D. Baker and John N. Wood

Molecular Nociception Group, Biology Department, University College London, Gower Street, London WC1E 6BT, UK

Mouse null mutants provide useful insights into gene function, but perinatal lethality or developmental compensatory mechanisms may obscure behavioural phenotypes. It is desirable to be able to delete genes in specific tissues, preferably in an inducible manner. The Cre-loxP system allows tissue-specific Cre-recombinase mice to be crossed with mice containing floxed (loxP-flanked) genes to produce tissue-specific null mutants. $Na_V1.8$ is a voltage-gated sodium channel expressed only in a subset of sensory neurons. More than 85% of these are nociceptors (e.g. Djouhri *et al.* 2003). We therefore inserted (knocked-in) the bacteriophage Cre-recombinase gene at the $Na_V1.8$ locus in embryonic stem cells and generated transgenic mice expressing Cre recombinase under the control of the $Na_V1.8$ promoter.

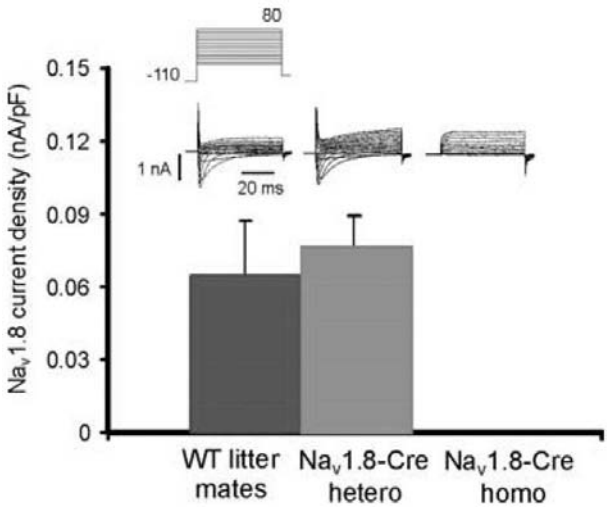

Figure 1. TTX-r transient currents are normal in $Na_V1.8$-cre heterozygotes, but abolished in $Na_V1.8$-Cre homozygotes. Mean $Na_V1.8$ current density is unchanged with the functional loss of one $Na_V1.8$ gene ($n = 22$, WT $n = 22$; means ± S.E.M.), whereas no transient TTX-r Na^+ currents were found in $Na_V1.8$-Cre homozygotes ($n = 26$). Inset: left, centre and right panels, example currents recorded from WT, $Na_V1.8$-Cre heterozygote and homozygote, respectively, in 250 nM TTX.

Analysis of the expression pattern of functional Cre recombinase using ROSA26 reporter mice demonstrated that Cre was expressed in an identical pattern to that of $Na_V1.8$. Expression began at embryonic day 14 in small diameter neurons in dorsal root, trigeminal and nodose ganglia, but was absent in non-neuronal or CNS tissues. This pattern of expression was unaltered in adult animals. Studies of $Na_V1.8$ heterozygous null mice have shown that these animals have normal electrophysiological and behavioural phenotypes (Akopian *et al.* 1999). $Na_V1.8$-Cre and wild-type (WT) mice were killed humanely and dorsal root ganglion cultures prepared. Tetrodotoxin-resistant (TTX-r) Na^+ channel expression in $Na_V1.8$ heterozygous Cre mice was indistinguishable from that in WT (Fig. 1). Similarly, thresholds of pain behaviour in response to thermal and mechanical stimuli in $Na_V1.8$-Cre heterozygotes and both phases of formalin-induced pain behaviour were identical in $Na_V1.8$-Cre heterozygotes and normal mice.

These findings demonstrate the $Na_V1.8$-Cre mouse line is a suitable tool to analyse the effects of gene deletion on pain behaviour. Specific gene deletion in nociceptors should provide insights into the role of broadly-expressed genes in nociception and pain pathways.

Akopian AN *et al.* (1999). *Nat Neurosci* **2**, 541–548.
Djouhri L *et al.* (2003). *J Physiol* **550.3**, 739–752.

The first two authors contributed equally to this work.

This work was supported by the MRC

All procedures accord with current UK legislation

C54

Peripheral inflammation produces a tonic EP1 receptor-mediated modulation of synaptic inputs to substantia gelatinosa neurones of the rat

V. Morisset, S.C. Lappin, C.H. Davies, G.M. Giblin and A.D. Randall

Neurology & GI CEDD, GlaxoSmithKline, Harlow, Essex CM19 5AW, UK

There is growing evidence that the antihyperalgesic effects of prostaglandin EP1 receptor antagonists in animal models of inflammatory pain are associated with spinal sites of action (Nakayama *et al.* 2002). In this study, we have examined the effects of two EP1 receptor antagonists (GW567675 and GW683868) on excitatory (glutamatergic) and inhibitory (glycinergic) synaptic inputs to substantia gelatinosa neurones *in vitro*.

For purposes of comparison experiments were performed on slices prepared from the spinal cords of two groups of rats. The first group were naive control animals, whereas the second group was composed of rats in which inflammation in the hind paw had been induced with a subcutaneous intraplantar injection of Freund's complete adjuvant (FCA), delivered approx. 24 h prior to electrophysiological data collection. Animals were humanely killed and spinal cord slices prepared from L4-L6 by standard means. After slice preparation standard whole-cell voltage-clamp recordings were performed at 32 °C on visualised substantia gelatinosa neurones. The holding potential was −60 or −70 mV for EPSCs and 0 mV for IPSCs. Corresponding miniature synaptic currents were isolated in 1 μM TTX. Data were compared using the Kolmogorov-Smirnov test and Student's *t* test. Statistical significance was assessed at $P < 0.05$.

In naive animals, neither GW567675 (1–10 μM) nor GW683868 (1–10 μM) altered the frequency of spontaneous glutamatergic EPSCs or IPSCs. In contrast, in FCA-inflamed animals, the EP1 antagonists significantly increased the frequency of spontaneous EPSCs in 5/10 cells (by 48 ± 14 %) and IPSCs in 6/13 cells (by 67 ± 9 %), respectively. Similarly, analysis of miniature synaptic currents revealed that EP1 antagonism significantly increased mEPSC frequency in 12/17 cells (by 67 ± 9 %) and glycinergic mIPSC frequency in 5/8 cells (by 73 ± 10 %), respectively. These changes in miniature frequency occurred in the absence of changes to the amplitude or kinetics of either the EPSC or IPSC population. The modulation afforded by EP1 antagonism was eliminated in the presence of 10 μM prostaglandin E2.

These data suggest a presynaptic location for prostaglandin EP1 receptors on the terminals of glutamatergic and glycinergic neurones. Following peripheral inflammation, these prostaglandin EP1 receptors become tonically activated by an endogenous ligand(s) which results in decreased synaptic release of both glutamate and glycine in substantia gelatinosa. This effect provides a potential cellular basis for the antihyperalgesic effects of prostaglandin EP1 receptors in inflammatory pain states.

Nakayama K *et al.* (2002). *Anaesthesiology* **97**, 1254–1262.

All procedures accord with current UK legislation

C55

Spinal vanilloid receptor-1 (TRPV1) becomes tonically active following peripheral inflammation

S.C. Lappin, M.J. Gunthorpe, A.D. Randall and V. Morisset

Neurology & GI Centre of Excellence for Drug Discovery, GlaxoSmithKline, Harlow, Essex, UK

The antihyperalgesic effects of TRPV1 receptor antagonists have been increasingly documented in animal models of both neuropathic and inflammatory pain. Although capsazepine has traditionally been used as an antagonist of these channels, its use is potentially problematic due to a limited selectivity and modality-specific antagonism. We have recently described the properties of a novel inhibitor of both recombinant and native TRPV1 channels SB-366791, which lacks many of the experimental liabilities of capsazepine, (Gunthorpe *et al.* 2004).

In the present study, we examined the effects of SB-366791 on glutamatergic synaptic transmission in substantia gelatinosa neurones within spinal cord slices prepared from male Lister-hooded rats, aged 17–26 days. Furthermore, we compared data from control rats and identical animals that have undergone a prior 24 h period of peripheral inflammation induced by an subcutaneous intraplantar injection of Freund's complete adjuvant (FCA) to the left hind paw. Following humane killing, 400 μm thick spinal cord slices were prepared from a region approximately encompassing L4-L6. Spontaneous excitatory post-synaptic currents (sEPSC) were then measured in whole cell voltage-clamp recordings of substantia gelatinosa neurones clamped at −70 mV.

In control animals, SB-366791 (30 μM) affected neither the amplitude (94.1 ± 2.4% of control, $n = 9$) nor frequency (99.4 ± 3.4% of control, $n = 9$) of sEPSCs. However, in 5/10 of FCA-inflamed animals, the addition of SB-366791 decreased sEPSC frequency to 66.3 ± 7.9% of its predrug level but produced no significant effect on sEPSC amplitude (92.2 ± 3.6% of control). Furthermore, the frequency of miniature glutamatergic EPSC (mEPSC), isolated in 1 μM TTX, from slices taken from FCA-treated animals was reduced by 30 μM SB-366791 in 6/7 animals (63.1 ± 4.2% of control values), without any corresponding change in the amplitude (95.7 ± 3.8% of control) of the mEPSC population.

These results suggest a presynaptic location for TRPV1 receptors on the terminals of glutamatergic neurones. We hypothesise that during peripheral inflammation TRPV1 receptors in sensory terminals become spontaneously active, resulting in an increased vesicular release of glutamate. These results provide new functional evidence for the involvement of TRPV1 in chronic inflammatory pain and provide a cellular basis for the antihyperalgesic effects of TRPV1 receptor antagonists.

Gunthorpe MJ *et al.* (2004). *Neuropharmacol* **46**, 133–149.

All procedures accord with current UK legislation

C56

Second messengers of octopamine receptors in the pond snail *Lymnaea stagnalis*

Samantha Pitt*‡, Agnes Vehovszky*†, Henriette Szabo† and Christopher Elliott*

** Department of Biology, University of York, York, UK and †Balaton Limnological Institute, Tihany, Hungary; ‡Present address: Department of Physiology, University of Cambridge*

We recently showed a major role for octopamine as a transmitter in the buccal ganglia of the snail *Lymnaea stagnalis* (Vehovszky & Elliott, 2001). Most octopamine responses in insects are mediated by adenylyl cyclase-dependent mechanisms (see, Roeder 1999 for review). To determine if this is also the case in molluscs, we recorded simultaneously the responses in the B1, B2 and B3 motoneurons to bath-applied octopamine in the presence of pharmacological agents which interact with the cAMP pathway.

The CNS was isolated and pinned down in a bath, though which saline was pumped at 1ml/min. Penetration of the visually identified neurons B1, B2 and B3 using glass micropipettes was assisted by application of 0.1 % protease (Sigma XIV). Signals were amplified and recorded to computer disk using DasyLab. Chemicals were dissolved in high Ca/high Mg saline or low Ca/high Mg saline, to reduce synaptically mediated background. Full details of the methods are given Vehovszky & Elliott (2001).

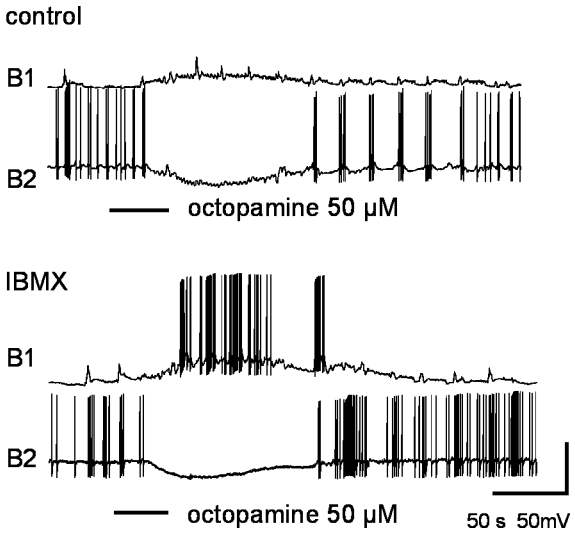

Figure 1. After 20 min 3-isobutyl-1-methylxanthine (IBMX, 50 μM) the response of the B1 motoneuron to 50 μM octopamine in the bath is much enhanced, while the response of the B2 motoneuron is unaffected.

The B1 motoneuron is depolarised by octopamine, with a threshold of 5 μM. The amplitude of the response is enhanced by preincubation for 20 min with 10 μM IBMX (an inhibitor of phosphodiesterase). Application of the direct cyclase activator 50 μM forskolin also depolarises the B1 motoneuron, but the inactive analog 1, 9-dideoxyforskolin has no effect. The membrane-permeable cAMP analog 8-bromo-cAMP also depolarise the B1 motoneuron, at 2 mM. Effects of the cyclase blockers SQ 22536 and Rp-cAMPS were only seen at extremely high concentrations (1–3 mM) – this may indicate that the tissue sheath or glial cells prevent these drugs from reaching the neurons. The response was also blocked by the G-protein Antagonist GDP-β-S. These observations are consistent with the hypothesis that the B1 has an octopamine receptor that activates adenylyl cyclase. The B2 and B3 neurons are hyperpolarised by octopamine – their thresholds are 5 and 0.5 μM respectively. Their responses are not affected by GDP-β-S, IBMX, 8-bromo-cAMP, Rp-cAMPS or SQ 22536. Forskolin has an excitatory effect on the B2 and B3 motoneurons; no inhibition was seen. In fact forskolin excites all the buccal neurons tested so far.

We conclude that the inhibitory octopamine receptor in the B2 and B3 neurons does not use cAMP for signalling, and must use a different pathway.

Vehovszky & Elliott (2001). *J Neurophysiol* **86**, 792–808.
Roeder (1999). *Prog Neurobiol* **59**, 533–561.

C57

Heterogeneous actions of cocaine and amphetamine regulated transcript (CART) peptides on rat sympathetic preganglionic neurones *in vitro*

M.J. Wall and D. Spanswick

Department of Biological Sciences, University of Warwick, Gibbet Hill Road, Warwickshire CV4 7AL, UK

The wide CNS distribution, neuronal co-localisation and profound actions following administration indicate that cocaine and amphetamine regulated transcript peptides (CART) play an important neuromodulatory role in the CNS. However the cellular actions of CART peptides remain largely unknown. Therefore we have begun to investigate the actions of CART peptides on sympathetic preganglionic neurones (SPNs) which receive direct inputs from both brainstem (Dun *et al.* 2002) and hypothalamic (Elias *et al.* 1998) neurones co-expressing CART.

Whole cell patch clamp recordings were made from neurones in transverse spinal cord slices from humanely killed neonatal Wistar rats (P7–14). SPNs were identified by their position in the lateral horn and characteristic electrical properties. The mean resting potential of SPNs was -54.5 ± 1.7 mV and the mean input resistance was 753 ± 39 mΩ, $n = 44$). In 4 SPNs, application of 200 nM rlCART (55–102) depolarised the membrane potential (from -48 ± 3.5 to -40.6 ± 4.1 mV) and reduced the neuronal input resistance. In a further 4 cells, 200 nM rlCART (55–102) produced a hyperpolarisation of the membrane potential (from -50.8 ± 3.5 to -55.3 ± 3 mV) and a reduction in input resistance (by 21.3 ± 5 %). The hyperpolarisation and decrease in input resistance were blocked by bicuculline (10 μM; $n = 2$) suggesting rlCART (55-102) activated $GABA_A$ receptors. In a further 30 SPNs, rlCART (55-102) had no action on the membrane potential or input resistance. The heterogeneous actions of CART peptides on SPNs may reflect the different CART inputs that these neurones receive: from the arcuate nucleus in the hypothalamus colocalised with POMC (α-MSH) and from the brainstem colocalised with noradrenaline. Thus we have compared the actions of α-MSH with those of rlCART (55-102). In 6 SPNs,

200 nM α-MSH depolarised the membrane potential (from −57.5 ± 2.7 to −47.5 ± 1.1 mV). However, unlike rlCART (55-102), the α-MSH induced membrane depolarisation was associated with an increase in input resistance (by 27.5 ± 7.5 %) suggesting the closure of resting conductances. In cells in which rlCART (55-102) induced membrane hyperpolarisation, α-MSH was without effect ($n = 3$) or produced a membrane depolarisation ($n = 1$).

These data suggest CART peptides differentially regulate electrical excitability of SPN. Further studies are required to clarify the functional significance of these observations and if these effects reflect differential CART inputs arising from the brainstem and hypothalamus.

Dun SL *et al.* (2002). *J Chem Neuroanat* **23**, 123–132.
Elias CF *et al.* (1998). *Neuron* **21**, 1375–1385.

All procedures accord with current UK legislation

C58

Effects of administration of SKF 38393, a D1 agonist, on methamphetamine-induced changes in shape of Zebrin bands in rat cerebellum

Mitsuko Hamamura, Takahide Shuto, Takao Shimazoe, Yasuyuki Fukumaki and Shigenori Watanabe

Department of Pharmacology, School of Pharmaceutical Sciences, and Division of Disease Genes, Institute of Genetic Information, Center for Bio-Regulation, Kyushu University Fukuoka 812-8582 Japan

The cerebellum is involved in emotional stress response and has parasagittal Zebrin (Aldolase C; Aldoc) bands expressed in Purkinje cells, which is thought to be a modular computing system (Brochu *et al.* 1990). Zebrin compartment has plasticity after external stimuli (Dusart *et al.* 1994; Zagrebelsky *et al.* 1997). We have reported by *in situ* hybridization study that daily methamphetamine administration (5 mg kg^{-1}, I.P.) for 3 days into rats induced fragmentation of Aldoc mRNA stripes and lateral shift of those stripes (Hamamura M *et al.* 1999). To know if these shape changes of Aldoc mRNA stripes are correlated with hyper locomotive behaviour induced by methamphetamine injections, we measured Aldoc mRNA in rats injected with a D1 receptor agonist SKF38393 (1 mg kg^{-1}, I.P.) for 1 week after prior injections (once 3 days for 2 weeks) of the methamphetamine (1 mg kg^{-1}, I.P.), whose treatment induced loss of hyper locomotion (Shuto *et al.* 2003). The rats were killed humanely.

The rats with the five injections of methamphetamine showed fragmentation of Aldoc mRNA stripe in the lobules VII and VIII. In addition, in the rats with the same repeated injections followed by the seven daily SKF38393 injections the number of stripes of Aldoc mRNA was not significantly different from those with repeated methamphetamine injections. On the other hand the shift of horizontal location of Aldoc mRNA stripes from the meridian in rats with repeated methamphetamine administration ($n = 4$ for each) was significantly different from either that in the saline control or that in the rats with methamphetamine plus SKF38393 treatment ($P < 0.05$, $n = 4$ for each, Wilcoxson's signed rank test). Since the SKF treatment rescued the horizontal shift of the Aldoc mRNA stripes induced by repeated methamphetamine injections, we conclude that the horizontal location change in Aldoc mRNA stripe but not the fragmentation is well correlated with behaviour in amphetamine psychosis.

Brochu G *et al.* (1990).) *J Comp Neurol* **291**, 538–52.
Dusart I (1994). *Neuroscience* **63**, 351–356.
Hamamura M *et al.* (1999). *Mol Brain Res* **64**, 119–31.
Shuto T *et al.* (2003). *Proc Am Soc Neurosci* **76**, 916.6.
Zagrebelsky M *et al.* (1997). *J CompNeurol* **379**, 283–99.

All procedures accord with current national and local guidelines

PC19

Dopamine D1 receptor modulation of rat striatal NMDA receptors

Huaxia Tong and Alasdair J. Gibb

Department of Pharmacology, University College London, London WC1E 6BT, UK

Striatal dopamine D1 receptors have been reported to increase (Flores-Hernandez *et al.* 2002), or attenuate NMDA receptor currents (Lee, *et al.* 2002). In our experiments we have used whole cell patch-clamp recordings from medium spiny neurons in 300μm thick striatal slices from humanely killed 7 day old rats to investigate the mechanism of NMDA receptor modulation.

NMDAR responses were evoked by 10 μM NMDA and 10 μM glycine. In the presence of TTX (100 nM) to block action potentials and the D2 receptor antagonist spiperone (2 nM) with ATP (1 mM) and GTP (1 mM) in the pipette solution. The D1 receptor agonist, SKF-82958 (20 nM), significantly (paired *t* test, $P < 0.05$) decreased the NMDA whole-cell current from 249 ± 36 pA to 153 ± 31 pA (mean ± S.E.M., $n = 10$ cells). Replacement of intracellular GTP with GDP-β-S (0.5 mM) did not prevent inhibition (control: 162 ± 34 pA, SKF-82958: 74 ± 12 pA, $n = 9$ cells) suggesting D1 inhibition is not dependent on G protein activation. These results are consistent with those of Lee *et al.* (2002) who demonstrated a direct inhibitory interaction between the C-termini of the D1 receptor and the NMDA receptor NR2A subunit. However protein immunohistochemistry (Portera-Cailliau *et al.* 1996) and *in situ* mRNA hybridization (Monyer *et al.* 1994) show a lack of NR2A expression in 7 day old rat striatum. We therefore tested for the presence of functional NR2A-containing receptors (Paoletti *et al.* 1997) using ZnCl2 (100 nM) or for the presence of tonic Zn inhibition using the Zn chelating agent TPEN (1μM) (control: 194 ± 20 pA, ZnCl2: 198 ± 15 pA, TPEN: 181 ± 11 pA, $n = 5$ cells).

These results suggest an absence of functional NR2A receptors in 7 day old rat striatum and therefore that there may be an NR2A-independent mechanism mediating direct, G protein-independent, inhibition of NMDA receptors in the neonatal rat striatum.

Flores-Hernandez J *et al.* (2002). *J Neurophysiol* **88**, 3010–3020.
Lee FJ *et al.* (2002). *Cell* **111**, 219–230.
Monyer H *et al.* (1994). *Neuron* **12**, 529–540.
Paoletti P *et al.* (1997). *J Neurosci* **17**, 5711–5725.
Portera-Cailliau C *et al.* (1996). *J Neurochem* **66**, 692–700.

This work was supported by the Wellcome Trust. H.T. is funded by a UCL Graduate School Research Scholarship

All procedures accord with current UK legislation

PC20

Functional effects of co-transfecting β-subunits 1, 1A and 3 with $Na_V1.8$ α-subunit in a COS-7 heterologous system

Mark D. Baker, W.-Y. Louisa Poon, John N. Wood and Kenji Okuse

Molecular Nociception Group, Department of Biology, Medawar Building, University College London, Gower Street, London WC1E 6BT, UK

$Na_V1.8$ is a tetrodotoxin-resistant (TTX-r) Na^+ channel that normally functions only in small diameter primary sensory neurones, and it is known to play a role in pain-pathways. The heterologous expression of peripheral nerve TTX-r Na^+ channels in mammalian systems has proved problematic, with low probabilities of functional expression and abnormal channel voltage-dependence and kinetics. We now know that poor expression may result from a requirement for accessory proteins, including the chaperone protein p11 (Okuse *et al.* 2002). However, Na^+ channel α-subunits in nerve are normally associated with β-subunits (e.g. Chen *et al.* 2002), and there is evidence that co-expression of $Na_V1.8$ with the $\beta1$ subunit increases functional expression when mRNA is injected into Xenopus oocytes (Vijayaragavan *et al.* 2001).

We have used lipofectamine to co-transfect green fluorescent protein (GFP, 0.4 μg) and an excess of cDNA for $Na_V1.8$ in pRK7 vector (0.7 μg), with and without one of 3 different β-subunits, 1 (0.7 μg), 1A (0.7 μg) and 3 (0.7 μg) in 7 μl lipofectamine into a COS-7 cell line cultured in 35 mm Petri dishes. The lipofectamine DNA suspension was in contact with the cells for 2 h before washing, and 48 h elapsed before recording from fluorescent cells began.

We found functional expression of $Na_V1.8$ in only 15.6% of fluorescent cells (total $n = 96$), when the α-subunit alone was transfected with GFP. There was no significant change in the probability of functional expression with $\beta3$ and $\beta1A$ subunits, but co-transfection with $\beta1$ reduced the probability to 2.2% (total $n = 45$, $P < 0.05$ Chi Square test, Yates corrected). The maximal Na^+ current density was unaffected by co-transfection of $\beta3$ (17.9 ± 5.73 pA pF^{-1} α-subunit alone, $n = 7$, *versus* 16.85 ± 1.85 pA pF^{-1} $\alpha + \beta3$ subunits, $n = 6$, means $\pm$ S.E.M.) however the average maximal current density was reduced by $\beta1A$ to 5.84 pA pF^{-1} ($n = 3$), although the effect was not statistically significant. The current voltage-dependence and kinetics appeared unchanged by the co-transfection of β-subunits, although the slope of the voltage-dependence of inactivation was non-significantly increased.

Our findings suggest that co-transfection of Na^+ channel β-subunits does not appear to be sufficient to recapitulate neuronal $Na_V1.8$ channel behaviour in a COS-7 heterologous expression system.

Chen C *et al.* (2002). *Proc Natl Acad Sci U S A* **99**, 17072–17077.

Okuse K *et al.* (2002). *Nature* **417**, 653–656.

Vijayaragavan K *et al.* (2001). *J Neurosci* **21**, 7909–7918.

We thank Lori Isom for the β-subunit clones. This work was supported by the MRC and the Wellcome Trust

PC21

Confocal imaging of isolectin B4 labelling as a tool for studying neuronal-capillary interactions in living cerebellar slices and retina from rats

Claire Peppiatt, Manuela Lahne, Clare Howarth, David Attwell and Peter Mobbs

Department of Physiology, University College London, Gower Street, London WC1E 6BT, UK

Understanding how neural activity regulates local cerebral blood flow is essential for understanding the BOLD signals detected in functional magnetic resonance imaging. Glutamate has been shown to dilate microvessels in slices of neocortex and hippocampus, and this may be mediated by NO release from neurons or by activation of astrocytes to release prostaglandins (Fergus & Lee, 1997; Lovick, 1999; Zonta *et al.* 2003). Studying regulation of microvessel diameter in living brain slices offers advantages in determining the mechanisms of vascular regulation (though with the disadvantage that the vessels are not perfused), but many vessels are not easily visible in brain slices. We have used isolectin B4 (Laitinen, 1987) from Bandeiraea simplicifolia conjugated to FITC (Sigma), which mainly recognises terminal α-D-galactosyl residues, to label the endothelial cells of blood vessels in cerebellar slices or retina from P7 and P15 rats (killed humanely by cervical dislocation). Since the lectin recognises an extracellular site, it can be used to label vessels in both living and paraformaldehyde-fixed slices. Z-stacks (100 μm in depth) of FITC fluorescence images at different depths of the cerebellar cortex or retina were acquired, thresholded to segment the image into labelled and non-labelled areas, and rendered using Zeiss LSM 510 software to construct a 3D rotatable image of the microvessel network.

At both P7 and P15 the cerebellar vascular network defined by isolectin B4 labelling was similar to that seen with India ink injection (Yu *et al.* 1994), although isolectin B4 also revealed microglia in the white matter. Arterioles penetrate the cerebellar cortex from vessels outside the folia, forming a dense network of vessels in the Purkinje cell layer and sending branches into the granular layer and molecular layers. Application of noradrenaline (2–100 μM) to living cerebellar slices or retina caused constriction of vessels in the vasculature network, however further work is needed to investigate whether binding of the lectin to the endothelial cells alters the control of microvessel diameter by neurotransmitters.

Fergus A & Lee KS (1997). *Brain Res* **754**, 35–45.

Laitinen L (1987). *Histochem J* **19**, 225–234.

Lovick T *et al.* (1999). *Neuroscience* **92**, 47–60.

Yu BP *et al.* (1994). *Acta Anat* **149**, 128–133.

Zonta M *et al.* (2003). *Nat Neurosci* **6**, 43–50.

This work was supported by the Wellcome Trust and a Wolfson-Royal Society Award.

All procedures accord with current UK legislation

PC22

Molecular and biophysical identity of orexin/hypocretin neurons

Denis Burdakov*, Haris Alexopoulos*†, Angela Vincent† and Frances Ashcroft*

*University Laboratory of Physiology and †Weatherall Institute of Molecular Medicine, University of Oxford, Oxford, UK

The orexin/hypocretin peptides are produced in neurons of the lateral hypothalamus which send widespread projections throughout the brain. Orexins are implicated in the maintenance of wakefulness and disruption of their function in animal models leads to narcolepsy (Hungs and Mignot, 2001). Recent *in vitro* experiments suggested that orexin neurons have intrinsic electrical pacemaker activity (Eggermann *et al.* 2003). Because orexin neurons are active principally during wakefulness, this intrinsic firing may be critical for the normal sleep-wake cycle. It is therefore of interest to elucidate the biophysical and molecular mechanisms responsible for the pacemaker activity of orexin neurons. Studies of other intrinsically firing neurons show that pacemaker activity arises from a complex interplay between plasmalemmal ionic conductances. Thus our aim was to characterise the molecular and biophysical determinants of ionic currents expressed by orexin neurons.

We performed standard whole-cell patch-clamp recordings in living brainslices of humanely killed mice (C57BL/6, male, P12–20) to elucidate the biophysical identity of these currents, by measuring the voltage-dependence of activation and the time- and voltage-dependence of inactivation, and their sensitivity to pharmacological agents. We also used multi-label immunocytochemistry combined with confocal microscopy to determine the molecular identity of the ion channel subunits which co-localise with orexin in lateral hypothalamic neurons. Together, these data allowed identification of currents which determine the firing properties of orexin neurons.

Eggermann *et al.* (2003). *J Neurosci* **23**, 1557–1562.

Hungs & Mignot (2001). *BioEssays* **23**, 397–408.

*The first two authors contributed equally to this work. This work is supported by the Wellcome Trust.

All procedures accord with current UK legislation

PC23

Targeting GABAergic neurones using an adenoviral vector

A.G. Teschemacher*, J.F.R. Paton†, D. Murphy‡ and S. Kasparov†

*Department of Pharmacology, University of Bristol, †Department of Physiology, University of Bristol and ‡Research Centre for Neuroendocrinology, University of Bristol, Bristol, UK

GABAergic neurones are involved in a vast variety of brain functions, including central control of arterial blood pressure. Visualisation of these cells is very difficult because of the lack of reliable antibodies. Moreover, none of the available stains are suitable for high quality fluorescence imaging of the fine structure of these cells. Visualisation of these neurones in live preparations has been attempted in a transgenic mouse where a short piece of the promoter of the GABA-synthesising enzyme GAD67 was used to drive EGFP expression in a subset of GABAergic cells in the hippocampus (Oliva, Jr. *et al.* 2000). Since the expression in other parts of the brain has not been well characterised and these animals are not readily accessible, we report here an alternative strategy for visualising living GABA interneurones within the brainstem.

We have generated an adenoviral vector that incorporates 3.7kb of the GAD67 promoter and the first exon-intron sequence to drive the expression of EGFP and tested the expression profile in brainstem and hippocampus. Male Wistar rats (75–150g) were anaesthetised (ketamine, 60 mg kg^{-1} and medetomidine, 250 μg/kg, ip) and bilateral injections of adenoviral vectors were made using fine glass capillaries. The rats were allowed to recover for 5–7 days and were then deeply anaesthetised (pentobarbitone 100 mg kg^{-1}, ip), perfused and brainstem sections processed for GABA using primary anti-GABA polyclonal antibodies and secondary rhodamine-coupled antibodies. In the hippocampus and nucleus tractus soliitarii (NTS) this vector resulted in medium-intensity EGFP expression in numerous neurones (soma size ~ 15–20 μm). In the hippocampus their location was consistent with the distribution of inter-neuronal layers. The absolute majority of EGFP-positive cells (> 90 % in NTS) were immunopositive for GABA. In addition, we have never observed EGFP expression in glial cells (< 10 μm) although some of these cells brightly stained for GABA presumably reflecting GABA uptake from the extracellular space. This vector has also been used to transfect putative GABAergic neurones in organotypic slice cultures of hippocampus and NTS. Fine details of these neurones were visualised using live cell confocal imaging. In conclusion, our novel vector is selective for GABAergic neurones, at least in certain brain areas. This approach will greatly facilitate imaging and electrophysiological studies centred on the role of GABAergic inhibition in physiological and pathological states.

Oliva AA Jr, (2000). *J Neurosci* **20**, 3354–3368.

Financial support: Royal Society (23697), BBSRC (7/JE616459), BHF (RG/02/011), WT (AL/069061).

All procedures accord with current UK legislation

PC24

Syntaxin-1A is excluded from recycling synaptic vesicles in cultured rat hippocampal neurons

Simon J. Mitchell and Timothy A. Ryan

Biochemistry Department, Weill Medical College of Cornell University, New York, NY 10021, USA

SNAREs (soluble NEM-sensitive factor attachment protein receptors) mediate the fusion of synaptic vesicles at the plasma membrane. The v-SNARE synaptobrevin is localised primarily to synaptic vesicles, although it redistributes onto the plasma membrane during vesicle recycling (Sankaranarayanan & Ryan 2000). Inversely, the t-SNARE syntaxin is thought to be anchored in the target plasma membrane. However, a cofractionation study showed that syntaxin-1 is also present in vesicular membrane (Walch-Solimena *et al.* 1995). We have investigated whether the subcellular distribution of syntaxin-1A is regulated during synaptic vesicle recycling.

Neurons were dissociated from hippocampal CA1-CA3 regions of 2-to 4-day-old Sprague-Dawley rats, which were killed humanely, and maintained in culture for 2–3 weeks prior to experiments. To monitor the distribution of syntaxin, we expressed super-ecliptic pHluorin (SE; Sankaranarayanan *et al.* 2000) fused to the C-terminus of syntaxin-1A (stx-SE). Data are presented as means ± S.E.M.

Under steady-state conditions, stx-SE was localised in somatic, dendritic and axonal regions. We quantified the subcellular localisation of stx-SE by monitoring fluorescence changes in stx-SE during either low pH or NH_4Cl application. We found that

$9 \pm 3\%$ ($n = 9$) of stx-SE at synaptic boutons (identified by FM 4–64 loading) was localised in an acidic compartment, which may correspond to synaptic vesicles (Walch-Solimena *et al.* 1995), while the remainder was on the presynaptic surface. At non-synaptic axonal regions, $100 \pm 2\%$ ($n = 9$) of stx-SE was present on the plasma membrane.

We next investigated whether intracellular presynaptic syntaxin was localised to synaptic vesicles that recycle during action potentials (AP). Repetitive AP stimulation at 10–100 Hz failed to induce accumulation or redistribution of stx-SE on the plasma membrane. Similar results were found when the signal-to-noise level was enhanced using prior photobleaching of baseline fluorescence and application of bafilomycin-A1, which blocks reacidification of recycling vesicles thereby trapping recycling stx-SE in a fluorescent form. These data indicate that syntaxin-1A is present in an internal compartment that does not participate in AP-evoked vesicle recycling.

Our results show that most syntaxin-1A is localised to the plasma membrane and remains excluded from synaptic vesicles during endocytosis. These data suggest that sorting of synaptic vesicle cargo from an abundant plasma membrane component operates with high fidelity.

Sankaranarayanan S *et al.* (2000). *Biophys J* **79**, 2199–208.

Sankaranarayanan S & Ryan TA (2000). *Nat Cell Biol* **2**, 197–204.

Walch-Solimena C *et al.* (1995). *J Cell Biol* **128**, 637–45.

SJM is in receipt of a Wellcome Trust International Research Fellowship.

All procedures accord with current national and local guidelines

PC25

Voltage-dependent sodium channel as a novel target controlled by metabotropic glutamate receptor via cAMP/PKA cascade in insect pacemaker neurones

C. Lavialle, F. Grolleau and B. Lapied

Laboratoire Récepteurs et Canaux Ioniques Membranaires (RCIM), UPRES EA 2647, Université d'Angers, UFR Sciences, 2 bd Lavoisier, F-49045 Angers cedex, France

Apart from the recently cloned metabotropic glutamate receptor (DmGluRA) from *Drosophila* melanogaster head cDNA library, the characterisation of the native neuronal mGluRs in insect is still in its infancy. Whole cell patch-clamp studies performed on the cockroach *Periplaneta americana* cultured adult dorsal unpaired median (DUM) neurones revealed that bath application of glutamate (10 μM) decreased the action potential amplitude. Under voltage-clamp conditions, both glutamate and the group III-selective mGluR agonist L-AP4 also reduced in a dose-dependent manner the voltage-dependent inward sodium current (I_{Na}) amplitude ($EC_{50} = 16.7$ nM and 760 nM, respectively). Because glutamate-mediated I_{Na} reduction was blocked by the group III mGluR antagonist MSOP ($IC_{50} = 45$ μM) and not by group I (AIDA) and group II (MCCG) mGluR antagonists, we concluded that a mGluR sharing pharmacological properties with the vertebrate mGluRIII was involved. Consistent with this, neither t-ADA nor LY354740, group I and group II-selective mGluR agonists respectively, induced any significant effect on I_{Na}. It is worth noting that the maximal inhibition of I_{Na} induced by glutamate and L-AP4 only reached $48.1 \pm 3.9\%$ (mean ± S.E.M., $n = 14$) and $33.5 \pm 4.1\%$ ($n = 6$), respectively. These results together with the deactivation tail current analysis showed that two sub-populations of voltage-gated sodium channels (Na1, Na2) were present in DUM neurones and only one (Na1) was sensitive to glutamate. We have also characterized the intracellular messenger pathway coupling this mGluRIII to Na1. The pertussis toxin A-protomer (10 nM), applied alone, decreased $I_{Na}1$ by $32 \pm 4.5\%$ ($n = 5$). In this condition, we never observed any effect of L-AP4. Increasing intracellular cAMP level, by perfusing the cell body with 0.3 mM cAMP through the patch pipette, also reduced $I_{Na}1$ ($28.44 \pm 4\%$, $n = 19$) like L-AP4. In this case, glutamate still produced an additional effect on $I_{Na}1$ as observed in control condition. Finally, because both glutamate and L-AP4 effects were completely suppressed in the presence of the PKA inhibitor H89 (0.3 mM), it was strongly suggested that glutamate regulated $I_{Na}1$ via a cAMP/PKA cascade. This was confirmed by immunocytochemistry using cAMP antibodies. cAMP immunoreactivity exhibited by DUM neurone cell body was observed before and after stimulating mGluRIII by glutamate and L-AP4. The intensity of the cAMP-immunofluorescence was higher with glutamate compared to L-AP4 demonstrating that the stronger effect observed with glutamate occurred via a higher elevation in cAMP level and suggested the implication of a second intracellular regulatory pathway.

C. Lavialle is supported by a doctoral fellowship from Region Pays de la Loire

PC26

Auditory pattern recognition based on instantaneous spike rate coding in the cricket (*Gryllus bimaculatus*)

B. Hedwig*, A. Nabatiyan*, J.F.A. Poulet* and G.G. de Polavieja†

Department of Zoology, Downing Street, University of Cambridge, UK-Cambridge CB2 3EJ and †Computational Neuroscience Group, Department of Theoretical Physics, Universidad Autónoma de Madrid, 28049 Madrid, Spain

Auditory pattern recognition by the CNS is fundamental to acoustic communication. For the neural processing of amplitude modulated sounds the instantaneous spike rate rather than the mean neural activity may be the appropriate coding principle. We compared both coding parameters in the simple auditory system of the cricket *Gryllus bimaculatus*. Since crickets communicate with stereotyped sound pulses (syllables) of constant frequency, they are established models to investigate the neuronal mechanisms of auditory pattern recognition. We demonstrate that the primary auditory afferents are not tuned to syllable patterns of certain repetition rates but they act as syllable onset detectors, which preferentially respond to the beginning of sound pulses. This explains why the duration of syllables is not relevant for phonotactic behaviour. When stimulated with different temporal sound patterns the response of a thoracic low order interneurone (Omega neurone ON1) is very similar when the average discharge rate is considered. However, analysing the instantaneous discharge rate, demonstrates that the neuron responds with prominent peaks in its instantaneous discharge rate to syllable rates close to the species-specific sound pattern. The occurrence and repetition rate of these peaks in the neuronal instantaneous discharge are sufficient to explain temporal filtering in the cricket auditory pathway since they closely match the tuning of phonotactic behaviour to different sound patterns. Temporal filtering or "pattern recognition" may not happen as previously proposed in the brain but may already occur at the earliest stage in the auditory pathway. This is in good agreement with robotic models of cricket phonotaxis, where pattern recognition results from simple low level auditory processing. Our data emphasize the importance of instantaneous discharge rate coding in auditory processing rather than integration of neural activity over long time periods.

This work was supported by a BBSRC research grant to BH (8/S17898)

PC27

Characterisation of electrophysiological consequences of traumatic brain injury in the rat using a novel *in vitro* model

D. P. Gitterman *, B. Morrison III ‡, L. E. Sundstrom † and C. D. Benham *

**Neurology & GI Centre of Excellence for Drug Discovery, GSK Research & Development Ltd, New Frontiers Science Park, Third Avenue, Harlow, Essex CM19 5AW, UK, † Department of Clinical Neurosciences, Bassett Crescent East, Southampton SO16 7PX, UK and ‡ Department of Biomedical Engineering, Columbia University, NY, NY 10023, USA*

White matter regions of the brain, which contain axonal tracts, have differing susceptibility to the consequences of traumatic brain injury (TBI) than regions containing predominantly neuronal cell bodies. Even relatively mild trauma, which does not immediately disrupt the axonal structure, can initiate processes that ultimately lead to the loss of axonal integrity and function. The changes in electrophysiological properties of neurons accompanying this degeneration remain to be fully understood. The work described here forms part of a European Union initiative aimed at reduced the number of *in vivo* experiments conducted in the field of brain injury. We have employed an *in vitro* model specifically designed to reproduce the brain deformation seen during rapid head deceleration associated with falls or road traffic accidents. To this end, organotypic hippocampal slice cultures (prepared from humanely killed 8 day-old rat pups) were grown on deformable silastic membranes. These were placed in a specially designed device which delivers precisely controlled and highly reproducible, equibiaxial stretch injury. Using slice cultures rather than dissociated neurons allowed the study of intact neuronal circuitry and using multi-electrode array technology enabled the behaviour of the whole network to be monitored simultaneously. Preliminary experiments show a time dependence of electrophysiolgical changes after stretch-injury. Input-Output relationships recorded in slices 4 h after injury are similar to sham-injured control tissue. After 48 h however, maximal EPSPs are substantially reduced (values represent mean electrode responses): control 0.55 ± 0.08 mV (S.E.M., $n = 7$), 4 h post-injury 0.52 ± 0.05 mV (S.E.M., $n = 7$) and 48 h post-injury 0.37 ± 0.05 mV (S.E.M., $n = 7$). Injury-induced effects were also seen when epileptiform bursting activity was evoked with the $GABA_A$ receptor antagonist bicuculline (10 μM). Bursting frequency dropped from 0.064 ± 0.007 Hz (S.E.M., $n = 6$) in control tissue to 0.031 ± 0.008 Hz (S.E.M., $n = 8$) 48 h after injury. In addition the proportion of ictal as compared to interictal bursting increased from $25.3 \pm 15\%$ (S.E.M., $n = 8$) to $54.7 \pm 15\%$ (S.E.M., $n = 9$) during the same period. These changes are being correlated with the time course of loss of neuronal viability as visualised by propidium iodide fluorescence.

All procedures accord with current UK legislation

PC29

Functional connectivity between the globus pallidus and subthalamic nucleus in a mouse brain slice preparation

K.C. Loucif*, C.L. Wilson†, M.G. Lacey† and I.M.Stanford*

** School of Life & Health Sciences, Aston University, Birmingham, B4 7ET; † Division of Neuroscience, The Medical School, University of Birmingham, B15 2TT, UK*

Reciprocal connectivity between the glutamatergic subthalamic nucleus (STN) and GABAergic globus pallidus (GP) appears essential for oscillatory activity and rhythmic bursting in the GP –STN network (Plenz and Kitai. 1999). This central pattern generator could play a prominent role in driving the oscillatory neuronal activity observed in several basal ganglia nuclei seen both in idiopathic Parkinson's disease and animal models thereof. Indeed, the frequency and pattern of this activity may be related to resting tremor. Here, we describe a brain slice preparation that maintains the functional connectivity between the GP and STN.

300–400 μm thick brain slices were obtained from 21–40 day old CB57BL/6JCrL mice. The animals were anaesthetised with fluorothane 4% in O_2 and humanely killed. Slices were continuously superfused with ACSF at 32–34 °C. Pellets of biocytin were implanted in either the GP or STN in slices prepared in the horizontal, saggital or parasaggital plane. After 8–10 h slices were fixed and processed to reveal the reaction product.

Extensive labelling, including fibres in the internal capsule and cell bodies in the GP and STN, together with labelling in substantia nigra and striatum, was best observed in parasagittal slices, reflecting both retrograde and anterograde biocytin transport. To show functional connectivity, whole-cell recordings were made in parasaggital slices cut 20° to the midline. Single shock stimulation in the GP evoked $GABA_A$ receptor-mediated IPSCs in the STN (44/59 cells) that reversed around E_{Cl} and were blocked by bicuculline (10 μM, $n = 7$). Stimulation of the STN evoked EPSCs in the GP (22/33 cells), which were blocked by CNQX (10 μM) and DL-AP5 (100 μM, $n = 5$). In 2/2 slices, both GP to STN and STN to GP connectivity was demonstrated. In current clamp, evoked EPSPs (from the STN) were able to trigger action potentials in the GP ($n = 3$), while evoked IPSPs (from the GP) caused a cessation of STN firing activity followed by a rebound depolarisation that was able to elicit further action potential firing ($n = 2$). Such rebound depolarisations in STN neurones could play a role in oscillatory activity.

In summary, the parasaggital mouse brain slice maintains functional GP-STN connectivity and provides a suitable model for future pharmacological and mechanistic studies of this basal ganglia neuronal network.

Plenz D & Kitai ST (1999). *Nature* **400**, 677–682.

This work was supported by a Parkinson's Disease Society (UK) Research Studentship (CLW), and the Wellcome Trust (Grant nos. 063461 & 068818).

All procedures accord with current UK legislation

PC30

Inhibition of I_h reduces epileptiform activity in rodent hippocampal slices

C.H. Gill, N. Shivji, J.T. Brown, S.C. Lappin, C. Farmer, N.C.L. McNaughton, A.D. Randall and C.H. Davies

Neurology & GI CEDD, GlaxoSmithKline, Harlow CM19 5AW, UK

The cationic anomalous inward rectifier current I_h has been suggested to be a pacemaker current controlling oscillatory activity in certain brain regions and recent evidence has proposed a role for this channel in epileptic states. We have therefore investigated whether I_h is critical in the generation of epileptiform discharges recorded from the adult hippcampal slice preparation, using extracellular electrophysiological techniques. The effect of the I_h blocker ZD-7288 was examined in a number of *in vitro* models of epileptiform activity, induced by a range of pharmacological manipulations.

Male Lister Hooded rats were humanely killed by cervical dislocation. Brain slices were prepared using standard methods and extracellular recordings were made from stratum pyramidale in hippcampal area CA3. Data are presented as mean ± S.E.M. ZD-7288 produced a concentration-dependent inhibition of both non-synaptic and synaptically-mediated epileptiform activity. Removing extracellular Ca^{2+} and elevating K^+ to 6 mM resulted in epileptiform activity which is independent of action potential driven synaptic activity. This non-synaptic bursting was partially inhibited by 10 μM ZD-7288 (32 ± 8 % reduction; $n = 5$) and completely abolished by 100 μM ZD-7288 ($n = 5$). Similarly, ZD-7288 produced a concentration-dependent inhibition of synaptically-mediated epileptiform activity in the following experimental models: removal of extracellular Mg^{2+} ($IC_{50} = 23 \pm 4$ μM; $n = 6$), elevation of extracellular K^+, from 3 to 8.5 mM ($IC_{50} = 27 \pm 7$ μM; $n = 3$–11) and the addition of 10 μM bicuculline to the extracellular medium ($IC_{50} = 18 \pm 7$ μM; $n = 5$). It has recently been reported that prolonged ZD-7288 application exerts a non-specific depression of glutamatergic synaptic transmission. Therefore we compared the time course of ZD-7288 inhibition of fEPSPs (recorded in area CA3 in response to stimulation in the dentate hilus) and epileptiform bursting induced by 10 μM bicuculline. At 30 and 60 mins after 100 μM ZD-7288 application a significant reduction in bursting frequency was observed without any significant change in fEPSP amplitude. A clear reduction in fEPSP amplitude was only observed after 120 mins, by which time epileptiform bursting had been abolished. Furthermore, capsazepine which exhibits similar potency to ZD-7288 at inhibiting I_h, failed to inhibit glutamatergic synaptic transmission *per se* (100 μM) but produced a significant inhibition of bicuculline-induced epileptiform activity (61 ± 8 %; $n = 7$ at 10 μM).

These data suggest that broad spectrum inhibition of I_h reduces neuronal hyperexcitability in the hippocampus and that molecules possessing this profile may be useful in treating temporal lobe epilepsy.

All procedures accord with current UK legislation

PC31

Extracellular recordings of a muscarinic excitatory postsynaptic potential in area CA1 of the rat hippocampus

J.P. Spencer, J.T. Brown and A.D. Randall

Neurology & GI CEDD, GlaxoSmithKline, Harlow, Essex CM19 5AW, UK

Acetylcholine (ACh)-mediated synaptic transmission in the CNS is a key component of mnenomic function and substantial cognitive deficits can be induced with cholinergic antagonists that penetrate the CNS. Furthermore, the most widely prescribed therapies for disease-related cognitive decline, such as that present in Alzheimer's disease, are agents designed to enhance cholinergic function. Despite this, relatively little work has been carried out on the neurophysiology of ACh-mediated synaptic responses in structures such as the hippocampus, which are central to normal mnemonic function. Using intracellular recording, a strongly desensitising muscarinic receptor-mediated EPSP has been recorded in hippocampal CA1 neurones in response to stimulation of stratum oriens (Morton & Davies, 1997). In this communication we describe extracellular recordings of this muscarinic EPSP and its modulation by pharmacological agents.

Male Lister-hooded rats were humanely killed by overdose of halothane, followed by decapitation, and hippocampal slices (400 μM thick) were prepared using standard methods. All recordings were made at approximately 32°C in a standard aCSF equilibrated with 95 % O2/5 % CO_2. To inhibit glutamatergic and GABAergic synaptic transmission the aCSF was supplemented with 10 μM NBQX, 50 μM D-AP5 and 10 μM Gabazine. Recording electrodes, filled with aCSF, were placed in stratum pyramidale of area CA1. Trains of four stimuli (100 Hz, 30–40 V, 30–60 μs duration) were applied to stratum oriens every 5 min using a bipolar stimulating electrode. These stimuli consistently produced a negative-going potential that increased in amplitude with stimulus number and/or strength. This response was excitatory in nature as it often drove post-synaptic firing. Application of the muscarinic antagonist atropine (10 μM) eliminated a substantial component of the response, although an initial early component sometimes remained. The atropine-sensitive component determined by subtraction rose slowly to peak (time to peak = 1.3 ± 0.2 s) and had a duration of approximately 10.3 ± 1.6 s ($n = 8$); a time course in good agreement with the previously reported intracellular recordings of a muscarinic EPSP (Morton and Davies, 1997). Application of the cholinesterase inhibitor physostigmine (10 μM) greatly enhanced both the amplitude (630 ± 199 % increase) and duration (273 ± 142 % increase, $n = 3$) of the atropine-sensitive component.

This study outlines a facile method to record population hippocampal muscarinic EPSPs and may prove valuable in understanding the regulation and plasticity of this physiologically important conductance.

Morton & Davies (1997). *J Physiol* **502**, 75–90.

All procedures accord with current UK legislation